

# Integrating courtyard microclimate in building performance to mitigate extreme urban heat impacts

Jesus Lizana <sup>a,b,c</sup>

Victoria Patricia López-Cabeza <sup>a</sup>

Renaldi Renaldi <sup>b,c</sup>

Eduardo Diz-Mellado <sup>a</sup>

Carlos Rivera-Gómez <sup>a</sup>

Carmen Galán-Marín <sup>a\*</sup>

<sup>a</sup> Departamento de Construcciones Arquitectónicas 1, Instituto Universitario de Arquitectura y Ciencias de la Construcción, Universidad de Sevilla, Avda. Reina Mercedes, 2, 41012, Seville, Spain

<sup>b</sup> Department of Engineering Science, University of Oxford, Parks Road, Oxford OX1 3PJ, United Kingdom

<sup>c</sup> Future of Cooling Programme, Oxford Martin School, University of Oxford, Oxford OX1 3BD, United Kingdom

\* Corresponding author. E-mail address: cgalan@us.es

## **Abstract**

Extreme heat events are expected to occur more often as a consequence of climate change. This paper quantifies the impact of urban climate on building performance and evaluates the benefits of specific microclimates, such as inner courtyards, to mitigate extreme heat impacts. A reference case study associated with two outdoor weather conditions, an inner courtyard and a local urban climate, was measured, simulated and validated in TRNSYS. The validated model was then compared to three building models with a single outdoor weather condition associated with the urban climate, weather data from a rural station and a typical year weather file. The models were evaluated in free-running conditions and with air-conditioning systems. The results show how urban climate can increase indoor discomfort hours by 32% in free-running conditions and demonstrate that courtyard microclimate can almost completely mitigate the impact of urban overheating in buildings, eliminating severe indoor discomfort hours by more than 88%. Moreover, the increase in cooling energy demand due to urban climate was reduced by more than 15% in the case of having air-conditioning systems. The findings manifest the importance of accurate weather data for building simulation and demonstrate how multi-nodal outdoor conditions can enable additional strategies to mitigate climate risks, highlighting urban microclimates as a promising strategy to tackle extreme heat events in buildings and cities.

**Keywords:** courtyard; microclimate; passive cooling; building simulation; local climate zone

## Nomenclature and abbreviations

AC	air-conditioning
ACH	air change rate, h <sup>-1</sup>
CV-RMSE	coefficient of variation of the root mean square error
DH	indoor discomfort hours, %
EBC	Energy in Buildings and Communities
EPBD	European Energy Performance in Buildings Directive
EPC	energy performance certificates
IEA	International Energy Agency
LCZ	local climate zone
MBE	mean bias error
NMBE	normalised mean bias error
PCM	phase change material
R <sup>2</sup>	coefficient of determination
RH	relative humidity
t	time
T	temperature, °C
TY	Typical year
UHI	urban heat island
WS	wind speed

### Greek letters

$\theta$	air temperature, °C
$\phi$	heat gains, W

### Subscript

Ap	Appliances
Int	Internal
Li	Lighting
Oc	Occupancy

## 1. Introduction

Global warming is increasing the risks of extreme heat waves, which are expected to occur more often and last longer (IPCC, 2014). The impacts of these climate-related extremes include alteration and irreversible impacts for people and ecosystems, increasing human morbidity (e.g., dehydration, heat stroke and heat exhaustion) and mortality (WMO and WHO, 2015). On a high-emissions pathway, the worst scenario related to very extreme heat waves in Europe is projected to occur in the low-altitude river basins and Mediterranean coasts of southern Europe, with its numerous densely populated urban centres (EEA, 2019). Moreover, the effects of heat waves will worsen in larger cities due to the urban heat island (UHI) effect. This will increase cooling demand in a classic feedback loop (Hong et al., 2020), with extreme summer temperatures in cities, up to 5°C higher than rural surroundings (IEA, 2018; Yenneti et al., 2020). Targets to climate-related hazards through resilience should be adapted to buildings in order to reduce and manage the climate risks and improve the comfort and well-being of citizens (United Nations, 2015).

For decades, the attention of researchers has mostly focused on the energy efficiency of buildings, as existing buildings play an important role in energy consumption and carbon emissions. Computer technology and building energy simulation tools have been combined with methods to compare the cost-effectiveness of energy conservation measures, which has been studied and debated for years. However, current simulation procedures present several challenges when addressing future building needs under climate change and urban climate projections, mainly related to weather data, metrics and urban microclimate, especially at the residential level (Bardhan et al., 2020). They are further detailed in the following paragraphs.

Firstly, the importance of weather data selection in building performance evaluations has been studied recently in different studies comparing rural meteorological stations and local climate zones (LCZs) (Yang et al., 2020); typical year (TY) weather files based on historical data and extreme weather conditions (Cui et al., 2017; Jiao et al., 2020; Siu & Liao, 2020); or TY weather files and future local climate projections (Mata et al., 2019; Shen et



al., 2019). The results prove that although building design procedures based on typical meteorological years provide a good representation of the long-term building energy performance and that these comparisons are reliable (Seo et al., 2010), they cannot effectively reflect the variation range and the overheating impact of LCZs. Some recent research proposes the creation of extreme year weather files in order to include more than a single TY of weather data in building simulations (Crawley et al., 2019; Nik & Arfvidsson, 2017). (Perera et al., 2018) even proposed a numerical model extending the building boundaries to include the urban context. The aim is to contribute to the impact assessment of climate change on buildings without neglecting the urban environment during extreme weather conditions, which will affect more frequently and intensely in the future (EEA, 2019). The optimal evaluation of the potential impacts and implications of these extreme urban weather conditions on building performance still requires further investigation.

Secondly, the metrics used in most of the building codes and energy performance certificate (EPC) procedures are based on energy and carbon indicators, and do not consider passive performance or thermal comfort indices. (Samuelson et al., 2020) evaluated the climate adaptation potential of buildings, highlighting how building regulations and incentive programs should look beyond energy as a sole performance metric of interest and consider passive survivability and thermal interactions with the urban climate in order to support climate-resilient building design efficiently. An example of alternative performance metrics was proposed by (Fiorentini et al., 2019), who defined an enthalpy-based index to measure the viability of ventilative cooling solutions. Other studies used adaptive comfort models in order to compare the effectiveness of passive measures (Bienvenido-Huertas et al., 2020). Moreover, other studies have shown how the trade-off between single passive performance and energy savings requires an additional statistical effort for an optimal design (Chi et al., 2020). (Lizana et al., 2019) evaluated passive cooling alternatives based on phase change materials (PCM) under free-running and idealised cooling conditions through a parametric analysis. They showed that PCM-based passive solutions specifically designed to reduce cooling energy demand using active systems could not improve building performance in free-

running conditions, even worsening indoor performance. This was produced because PCM with melting temperature specifically configured for active cooling applications will be fully melted during warm free-running periods, overheating, even more, the indoor space since PCM cannot release latent heat stored. (Serrano-Jiménez et al., 2019) demonstrated how building performance differs according to the energy-related occupant behaviour, showing high imbalances in the results offered by official procedures for retrofitting criteria. These previous studies demonstrate the need for standardised comfort metrics in official procedures to guarantee the mitigation of heat impact in buildings.

Thirdly, the benefits of specific urban microclimate environments, such as inner courtyards, are not considered by current decision-support tools, which can mitigate the impact of extreme heat conditions in buildings (Rojas-Fernández et al., 2018). (Zamani et al., 2018) and (Rivera-Gómez et al., 2019) showed how inner courtyards are a powerful urban microclimate alternative for passive cooling. Courtyard microclimate has been used for thousands of years in different climates worldwide (Taleghani, 2014). Their benefits were previously quantified from different evaluation approaches. For example, (Natanian et al., 2019) and (Natanian & Auer, 2020) evaluated the energy and environmental performance of a set of urban configurations through a digital workflow using EnergyPlus, Radiance and ENVI-met simulation engines, showing that among the block typologies, the courtyard typology achieved the optimal combination among the environmental criteria tested. (Rivera-Gómez et al., 2019) evaluated the performance of 20 different courtyards in Spain, showing how some courtyard configurations can decrease extreme heat temperature by up to 15°C. (Diz-Mellado et al., 2021), (V.P. López-Cabeza et al., 2021) and (Sánchez de la Flor et al., 2021) have provided different numerical approaches to model the courtyard microclimate. Moreover, various studies have demonstrated how courtyard microclimate performance can be improved through different techniques, such as the use of shading devices (Victoria Patricia López-Cabeza et al., 2018), the variation of surface reflectance (Kristian Fabbri et al., 2020), the introduction of vegetation (Altunkasa & Uslu, 2020) or the modification of aspect ratio (Lopez-Cabeza et al., 2020), among

others. These specific microclimates can solve the problem of the urban overheating effect, mitigating peak daytime temperatures and promoting higher air change (ACH) rates at night (cross ventilation) to cool down the indoor environment (Zhou et al., 2020).

Despite the benefits described, courtyard performance is never considered in building performance by existing building energy simulation (BES) tools or white-box models (Li et al., 2021), such as EnergyPlus, eQuest, TRNSYS, ESP-r, etc. Even though a calibrated and relatively accurate baseline building model can be achieved through the collection of a relatively complex set of input data (Coakley et al., 2014), the integration of courtyards as a climate-resilient solution to mitigate heat impacts in buildings requires the application of multiple outdoor weather conditions, not available in existing procedures. Most of the microclimate studies related to inner courtyards and other urban microclimates are focused on CFD-based modelling (K. Fabbri & Costanzo, 2020; Forouzandeh, 2018; V. P. López-Cabeza et al., 2018), without considering the influence on building performance. Moreover, the currently available weather datasets used in building simulation software are mainly obtained from weather stations located in remote or rural areas (Chan, 2011). This means that the impact of the urban climate or specific microclimates on buildings' thermal and energy performance cannot be effectively evaluated. There is a need to update the regulatory framework and procedures to support the decision-making process towards climate-resilient building design, implementing a holistic climate-resilient approach to achieve a sustainable climate change adaptation of cities.

This research aims to evaluate the impact of urban climate on building performance and quantify the benefits of specific urban microclimate configurations, such as the inner courtyards, to mitigate the extreme heat impact. A reference case study associated with two outdoor weather conditions, an inner courtyard and a local urban climate, was measured, simulated and validated in TRNSYS. The building performance was then compared with three building models with a single outdoor weather condition, related to the LCZ climate affected by urban overheating, weather data from a suburban station and a typical meteorological year weather file for the region.

The building models are compared in free-running conditions through indoor discomfort hours (%) using the adaptive comfort model and with idealised air-conditioning (AC) systems through cooling energy demand (kWh/m<sup>2</sup>). There are mainly three research contributions in this work supporting the three research gaps previously mentioned:

- The implications of weather data selection in building performance in a hot climate in Europe are highlighted by comparing different outdoor datasets based on TY weather files, rural weather data and urban climate affected by urban overheating.
- The need for additional metrics in building codes and building performance certificate procedures to face future building needs under extreme heat events is evaluated. Some energy conservation measures, such as higher insulation or lower infiltration rates, have provided positive or negative benefits during extreme climate periods when comparing performance indicators based on passive building performance with energy efficiency metrics. The implementation of passive performance metrics, such as the percentage of indoor discomfort hours in free-running conditions (without air conditioning systems), has been shown to be necessary to improve the passive survivability of buildings.
- Finally, the potential benefits of specific microclimates on building performance, such as inner courtyards, are experimentally evaluated and numerically quantified to promote climate-responsive building design. The proposed numerical simulation approach, based on integrating multi-nodal outdoor conditions in building performance simulation, enables the development of additional passive cooling strategies in buildings based on urban microclimates.

These contributions provide novel criteria to correctly update future building codes and policies looking beyond energy efficiency targets towards a climate-resilient pathway. They support considering more appropriate weather data, comfort metrics and urban microclimate strategies to improve building performance under extreme weather events.

The paper is structured as follows. First, scenarios of urban climates and microclimates affecting building performance are introduced and characterised. Second, the approach for the evaluation of building performance is detailed for each climate scenario. Finally, the results are presented and discussed, showing the impact of different weather datasets on building performance and the benefits of courtyard typology to mitigate urban overheating.

## 2. Urban climates and microclimates affecting building performance.

The building performance in the same urban context under different climate situations is evaluated through four scenarios, illustrated in Fig. 1. These are listed from the most realistic case (Scenario 1), which considers the urban climate and microclimate affecting the building, to the standardised building evaluation using a TY weather file (Scenario 4).

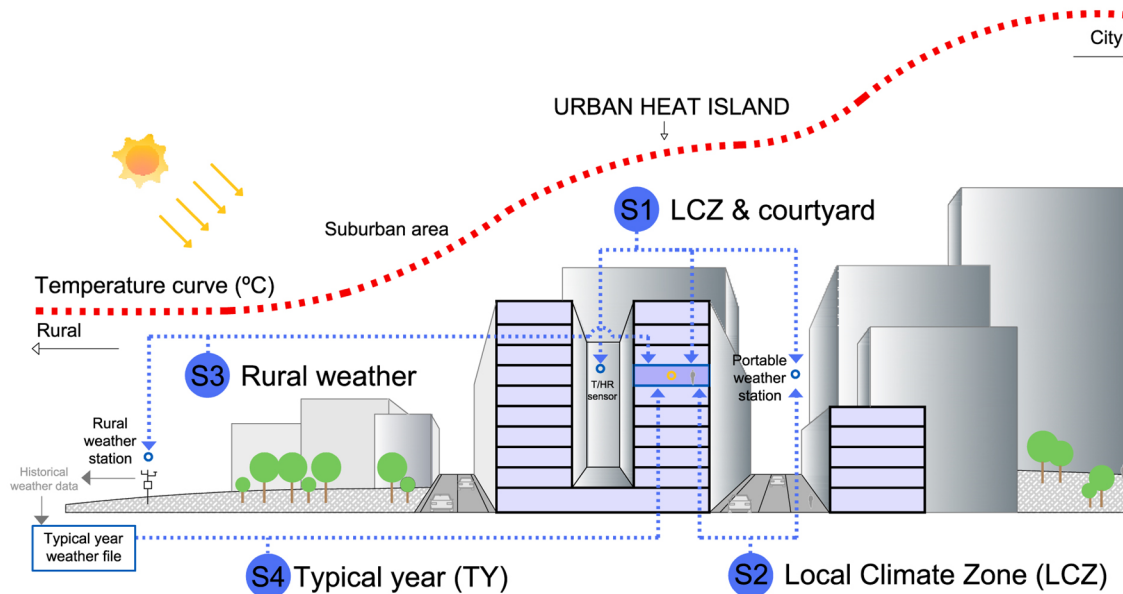


Figure 1. Building modelling scenarios under different urban climates.

Scenario 1 (S1) represents the building performance associated with two outdoor climate nodes: the urban climate or LCZ, affected by urban overheating, and the courtyard microclimate.

Scenario 2 (S2) consists of the building associated with a single outdoor weather node for the urban climate. In this case, the potential benefits of courtyard microclimate to mitigate heat impacts are not considered.

Scenario 3 (S3) shows the building linked to a rural or suburban weather condition, without the impact of urban overheating. These weather conditions represent the most widespread data sources for weather file generation, which are obtained from official meteorological networks located in rural or suburban areas and do not represent urban climate (Tsoka et al., 2018). In this case, the weather dataset is based on the period in which the case study was monitored, corresponding with a specific climatic situation of the study period.

Scenario 4 (S4) evaluates the building performance using the most extended TY weather file used for building simulation from the EnergyPlus database (*EnergyPlus. Weather Data for simulations*, n.d.). These data sets are created using historical weather data from long periods (at least 10 years) provided by official meteorological stations, most of them outside the urban centres. Thus, these files present average weather conditions which do not adequately represent urban climate (Tsoka et al., 2018) and changing and extreme climate events (Cui et al., 2017).

This study evaluates the importance of accurate weather data for building performance evaluations by comparing the thermal performance of a representative building model using these different weather datasets. The results discuss the viability of TY weather files for supporting a climate-resilient building design; evaluating the impact of urban climate in building performance in comparison with suburban weather conditions; and quantifying the potential benefits of specific urban microclimates, such as inner courtyards, to mitigate the extreme heat impact in buildings.

### **3. Materials and methods**

The methodology for building model simulation under different climate scenarios is divided into five sections. First, the reference case study is defined and characterised. Second, the numerical model for building simulation is detailed. Third, weather datasets used for each building scenario are explained. Fourth, the procedure for model calibration and validation is detailed. Finally, the building performance indicators used to evaluate the impact of each scenario are described.

#### **3.1. Reference case study**

A representative building typology in southern Europe was selected as a reference case study (Instituto Nacional de Estadística, 2011). This consists of a dwelling unit in a multi-family block of apartments in Seville (Spain), whose location and configuration are illustrated in Fig 2. The building is located in an urban context classified as open midrise (LCZ-5) according to the urban climate classification system proposed by (Stewart & Oke, 2012).

The metropolitan area of Seville, with more than 1.5 million inhabitants (INE, 2013), is the fourth most populated metropolitan area in Spain and a major tourist, economic, industrial and population centre. Seville enjoys a characteristically Mediterranean climate, with relatively mild winters and very warm summers. The Köppen Climate Classification subtype for this climate is "Csa" (Mediterranean Climate) (Chen & Chen, 2013; Köppen climate classification, n.d.). In this region, according to (AEMET, 2019), a heat wave period is considered an episode of at least three consecutive days with maximum temperatures above the threshold corresponding to the 95th percentile of daily maximum temperatures, whose value is 41.2°C for Seville considering the period from 1971 to 2000. Recent studies show an increasing occurrence of heat waves in the region in the last decade (AEMET, 2019; EEA, 2019). Since 1975, 20% of these phenomena have occurred in the previous five years in Seville (AEMET, 2020). And even 37% have occurred in the last decade considering the whole of Spain (AEMET, 2019; EEA, 2019). Moreover, the annual mean trendline of maximum temperature in Seville is increasing by 0.34°C per decade (*Hothaps-Soft. Climate Data and Heat Exposure Software*, 2014; Kjellstrom et al., 2009).



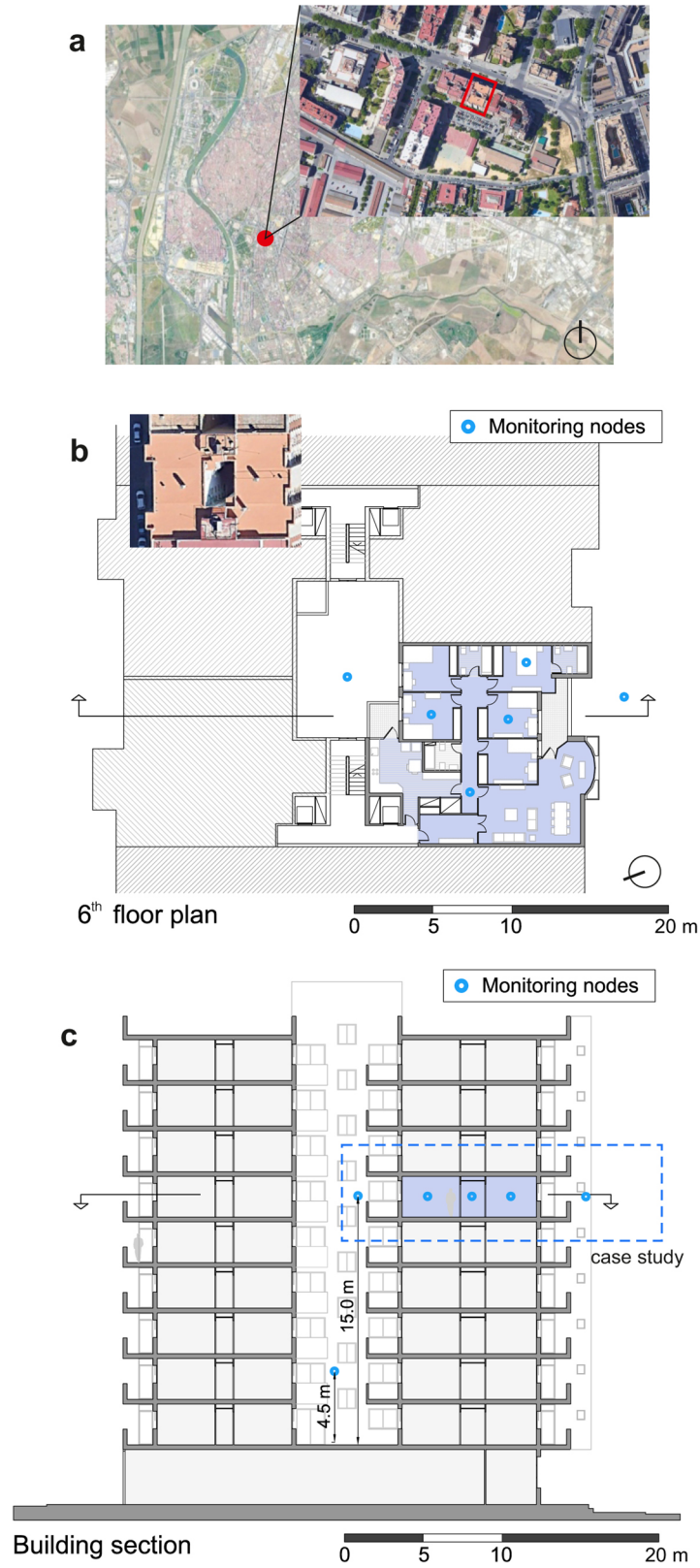


Figure 2. Selected reference case study with courtyard microclimate. a, Location in Seville. b, Floor plan. c, Building section.

The case study consists of a nine-storey block built in 1983, which implemented the first national regulation for thermal conditions and energy demand requirements for heating and cooling in buildings (NBE-CT-79, 1979). Almost 34% of the housing stock is still based on this building regulation (Instituto Nacional de Estadística, 2011). The selected residential unit has a floor surface of 136m<sup>2</sup> on the sixth storey (Fig. 2b), at approximately 15 m above the courtyard floor (Fig. 2c).

The case study was initially characterised through technical audits and occupant behaviour questionnaires. Table 2 summarises the main constructive element parameters of the residential unit.

*Table 2. Characterisation of the constructive elements of the reference case study.*

<b>Element</b>	<b>Definition</b>	<b>Characterisation</b>
Window 1	Double glazing system (4-6-4mm) with aluminium frame	U-value: 2.29 W/m <sup>2</sup> K
Window 2	Single glazing system (6mm) with aluminium frame	U-value: 5.69 W/m <sup>2</sup> K
Façade	Cement mortar, ceramic brick, insulation, air chamber, hollow brick, plaster (27cm)	U-value: 0.74 W/m <sup>2</sup> K
Internal wall	Plaster coating, ceramic brick, plaster coating (14cm)	U-value: 2.92 W/m <sup>2</sup> K
Internal partition	Plaster coating, hollow bricks, plaster coating (7cm)	U-value: 2.92 W/m <sup>2</sup> K
Internal floor	Terrazzo flooring, concrete slab, plaster coating (30cm)	U-value: 2.11 W/m <sup>2</sup> K

The dwelling has a heat pump for AC in the living room, which was not working during the monitoring period. Thus, the model was monitored, simulated and calibrated in free-running conditions.

### **3.2. Numerical model for building simulation**

The building was numerically modelled using the energy system simulation software TRNSYS v18. The dwelling case study was modelled as a multi-zone and implemented in TRNSYS Simulation studio using TYPE 56. The model geometry, illustrated in Fig. 3, reproduces the existing form, window surfaces (blue surfaces), and external shadings (purple surface).

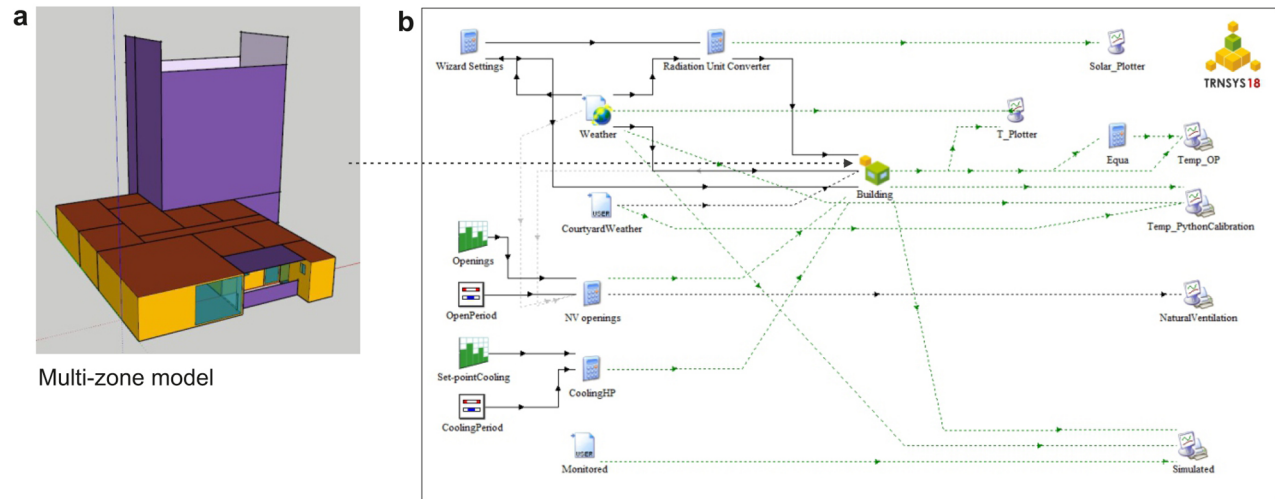


Figure 3. Numerical model for building simulation. a, Building model reproducing case study geometry, windows and shadings. b, Process flowsheet of the numerical simulation model developed in TRNSYS v18.

Reference handbooks, standards and related building codes supported the building parameterisation. Additionally, an iterative calibration process was addressed to reduce the number of uncertain input parameters, defined in section 3.4. The procedure, references and final parametrisation values are detailed below.

The dwelling was numerically characterised in TRNSYS through TRNBuild, including building elements (walls, floors, ceilings, roofs and windows), internal gains and schedules, infiltration and ventilation rates, among other aspects. Boundary conditions of the ceilings, floors and party walls were defined as identical.

Heat flow rates of internal gains were divided into occupants ( $\Phi_{int,oc}$ ), lighting ( $\Phi_{int,li}$ ) and appliances ( $\Phi_{int,ap}$ ). The heat flow from occupants was calculated following the procedure defined in Annex C of (EN 16798-2, 2019). Apartment buildings were characterised with an average metabolic rate of 1.2 met (ISO 7730:2005, 2005), which resulted in a dry and total heat loss per occupant of 80.3 W and 118.3 W, respectively. Different daily occupant schedules were considered for weekdays and weekends according to real building usage. The sensible heat gain from lighting was calculated according to the total electrical input power, the power dissipated by control gear and lighting use (ASHRAE Handbook - Fundamentals, 2017; CIBSE, 2007; EN 15193-1, 2017). Lighting heat gains ranged from 0 to 2.0 W/m<sup>2</sup> according to daily lighting schedules. The total heat flow rate of appliances

for residential buildings was defined at 3 W/m<sup>2</sup> according to (EN 16798-1, 2019). All heat flow schedules were determined according to real building usage, measured data and reference residential profiles defined in (EN 16798-1:2019, 2019).

Infiltration leakage is defined by an ACH rate of 0.6 h<sup>-1</sup>. This value was first estimated according to the procedure defined in (IDAE, 2012) taking into account the building typology, construction year, interior building volume, window area and permeability of the frames (EN 13465, 2004; EN 16798-7, 2017); and then calibrated according to real indoor air temperature oscillation. This value lies within the range of typical ACH rates of similar buildings built in the 1980s in southern Europe (Escandón et al., 2017; Fernández-Agüera et al., 2019; Vazquez Otero, 2016) and the reference values for multi-family buildings with low leakage levels reported in (EN 15242, 2007) and CIBSE Guide A (CIBSE, 2007).

Ventilation due to window openings was incorporated into the building model using the new simplified calculation method for natural ventilation (Eq. 1) introduced by EN 16798-7:2017 (EN 16798-7, 2017). Previous expressions with different levels of detail were proposed by De Gids and Phaff (1982) (De Gids & Phaff, 1982), Warrens & Parkins (1985) (Warren, 1977; Warren & Parkins, 1985) and Larsen (2006) (T. S. Larsen, 2006; Tine S. Larsen & Heiselberg, 2008). In this case, the new version proposed consists of a modified version of De Gids and Phaff (1982) (De Gids & Phaff, 1982), previously implemented in standard (EN 15242, 2007), and modified in the new EPBD standard (EN 16798-7, 2017) for the determination of natural airflow rates in buildings. This calculation method ensures that the associated airflows are based on building physics, involving window opening area profiles, air temperature difference, wind velocity and turbulence near the opening (Plesner et al., 2016). This reflects a fair evaluation of different ventilation situations (IEA EBC Annex 62, 2018; Plesner et al., 2016) according to the working group of IEA EBC Annex 62 on Ventilative cooling (IEA EBC Annex 62, n.d.).

$$q_v = 3600 \cdot \frac{\rho_{a,ref}}{\rho_{a,ext}} \cdot \frac{A_{w,tot}}{2} \cdot \max \left( c_{wnd} \cdot u_{10;site}^2; C_{st} \cdot h_{w,st} \cdot abs(T_z - T_e) \right)^{0.5} \quad (1)$$

where:

$q_v$ : airflow through the window ( $m^3/h$ )

$\rho_{a,ref}$ : air density at sea level, 293 K and dry air ( $1.204 \text{ kg/m}^3$ )

$\rho_{a,ext}$ : external air density [ $kg/m^3$ ]

$A_{w,tot}$ : total window opening area ( $m^2$ )

$c_{wnd}$ : coefficient taking into account wind speed in airing calculations ( $0.001 \text{ 1/(m/s)}$ )

$u_{10;site}^2$ : wind velocity on site

$C_{st}$ : Coefficient taking into account stack effect in airing calculations ( $0.0035 \text{ (m/s)/(m}\cdot\text{K)}$ )

$h_{w,st}$ : useful height for stack effect for airing [ $m$ ]

$T_z$ : air temperature of the ventilated zone [ $K$ ]

$T_e$ : external air temperature [ $K$ ]

The natural ventilation model was implemented in TRNSYS through an equation tool along with a daily profile for window opening area, defined and iteratively calibrated according to real building usage and measured data, simulating the day-to-day manual control of natural ventilation. Moreover, air coupling (or zone-to-zone air changes) was defined and iteratively calibrated, considering measured indoor conditions per zone.

Thermal bridges were considered through a default allowance of  $0.10 \text{ W/m}^2\text{K}$  of envelope area as defined in ISO 13789:2017 (ISO 13789:2017, 2017) for the case of existing buildings where details are not known.

The internal heat capacity of construction elements is directly integrated into the layers defined in TYPE 59. The internal heat capacity of air and furniture in the building model was calculated by multiplying the indoor air volume thermal capacitance of the model (in  $\text{kJ/K}$ ) by a constant value (Lizana et al., 2019). The multiplier should range from 3 to 5 according to the TRNSYS software guideline (*TRNSYS 18 Technical Documentation. Volume 9: Tutorials*, n.d.) or from 3 to 8 according to (Johra & Heiselberg, 2017). In this case, assuming a low furnishing density, the multiplier was fixed at 5 in order to consider a furnishing heat capacity of  $13 \text{ kJ/m}^2\text{K}$ . This value is between the reference value of  $17 \text{ kJ/m}^2\text{K}$  provided by (Johra & Heiselberg, 2017) for low furnishing density and the value of  $10 \text{ kJ/m}^2\text{K}$  provided by (ISO 52016-1, 2017).

### 3.3. Weather data for different scenarios

This section describes the weather data source for numerical modelling used per building scenario, summarised in Table 1.

Table 1. Summary of weather files and data source used for building modelling scenarios.

Scenarios	Outdoor nodes	Definition of climate nodes	Weather data source (equipment)	Variables (Accuracy)
S1. LCZ & Courtyard	2	LCZ-5 and courtyard microclimate	Portable weather station (PCE-FWS 20) Sensor in inner courtyard at 15.0 m (TESTO 174H) Seville weather station (WMO 083900)	T ( $\pm 0.5$ °C), RH ( $\pm 3\%$ ) WS ( $\pm 1$ m/s, 10%) Solar radiation (-)
S2. LCZ	1	LCZ-5	Portable weather station (PCE-FWS 20) Seville weather station (WMO 083900)	T ( $\pm 0.5$ °C) RH ( $\pm 3\%$ ) WS ( $\pm 1$ m/s, 10%) Solar radiation (-)
S3. Rural weather	1	Weather data in rural area	Seville weather station (WMO 083900)	T (-) RH (-) WS (-) Solar radiation (-)
S4. Typical year	1	TY weather file based on historical weather data	IWEC data file derived from historical weather data for 1992-1999. EnergyPlus database ( <i>EnergyPlus. Weather Data for simulations</i> , n.d.)	T (-) RH (-) WS (-) Solar radiation (-)

Sensors were separated from walls at a distance higher than 0.5 m to avoid possible data contamination by surface temperature.

Scenario 1 simulated the building facing two outdoor climate nodes: the LCZ and the inner courtyard. Air temperature (T), relative humidity (RH) and wind speed (WS) in the urban environment (LCZ-5) were monitored with a portable weather station (PCE-FWS 20). The courtyard microclimate was measured using data loggers (model TESTO 174H), widely used in previous studies (Diz-Mellado et al., 2021; Rivera-Gómez et al., 2019), protected with naturally ventilated radiation shields to protect the sensors and improve the accuracy of the measurements during the daytime, avoiding overheating. The outdoor sensors were located 15 m above the courtyard floor, as illustrated in Fig. 2, and were installed at least 0.5 m away from the wall to avoid possible data contamination by surface temperature and at least 1.5 m away from windows to avoid outgoing airflow conditions. Data were recorded from 01st June 2020 to 31st August 2020. During this period, ten days achieved maximum air temperatures in the urban environment higher than 41.2°C, which supposes 95% percentile from 1971-2000 (AEMET, 2019), representing an extreme urban weather condition. Sensors have an accuracy of  $\pm 0.5$  °C and  $\pm 3\%$  for temperature and relative humidity, respectively. The logging interval was defined every 15 minutes, and quality control procedures were applied, including plausible value and time consistency checks. Final datasets were generated on an hourly basis. Additionally, hourly solar radiation values (global horizontal, direct normal and diffuse radiation) were collected from Seville's suburban official weather station (WMO 083900).

The courtyard surfaces facing the courtyard microclimate node were numerically modelled as an equivalent resistance layer with a boundary condition linked to the courtyard air temperature dataset at 15.0 m. Additionally, solar radiative and convective gains of zones in contact with the inner courtyard were previously obtained by simulating the zones as external, and then manually introduced as hourly heat flow input value per zone. This numerical procedure, used to model the impact of a second outdoor microclimate in the building simulation, was verified using the same external conditions in both weather nodes, obtaining an identical behaviour. This modelling approach was then calibrated and validated using measured data. The following building scenarios are based on the same calibrated building numerical model (see section 3.4), in which just weather datasets are modified as follows.

Scenario 2 only considers the weather data obtained by the portable weather station (PCE-FWS 20) in the urban climate (or LCZ) in both outdoor nodes previously defined. Thus, in this case, there is no consideration of courtyard microclimate. The selected urban climate is classified as open midrise (LCZ-5) (Stewart & Oke, 2012) and is characterised by a skewed urban configuration that favours heat accumulation (Ratti et al., 2006; Xu et al., 2021). This LCZ is the most extended in the city.

Scenario 3 was evaluated using weather data from the nearest official AEMET (National Meteorological Agency in Spain) weather station in Seville (WMO 083900), which is located in a rural/suburban area (Government of Spain, 2019).

Scenario 4 assesses the building performance using the most extended TY weather file of the region for the same timeframe. The weather dataset was obtained from EnergyPlus database (*EnergyPlus. Weather Data for simulations*, n.d.) and consists of an IWECC1 data file for Seville developed by ASHRAE in 2001. The files were derived from up to 18 years (1982-1999 for most stations) of archived hourly weather data from the US National Climatic Data Center. These TY weather files are an artificial hourly weather year created with historical weather

data reflecting long-term average conditions for a location (Seo et al., 2010). They have been widely used and are useful for predicting energy consumption closer to the long-term average.

All building scenarios are modelled with the courtyard shadings. Weather datasets for scenarios 1, 2 and 3 have the same solar radiation values obtained from the rural weather station of Seville.

### **3.4. Model calibration and validation**

The numerical model was calibrated through an iterative simulation process integrating TRNSYS with a Python script to reduce uncertainties in input parameters, whose workflow is illustrated in Fig. 4. After each simulation, the Python script compares the measured data (Fig. 4a) with simulated values (Fig. 4b), automatically calculating recommended statistical indices for model validation (Fig. 4c), following the criteria defined by ASHRAE Guideline 14-2014 (ASHRAE, 2014). The boundary conditions of scenario S1 were used for model calibration and validation since it considers the most realistic building performance. This building modelling scenario includes two outdoor weather nodes for the simulation: the courtyard microclimate and the urban climate. The calibration was developed during the monitored period from 01st June 2020 to 31st August 2020. Fig. 4c also shows the results of the final performance of the validated model (orange lines) in comparison with measured data (blue lines).



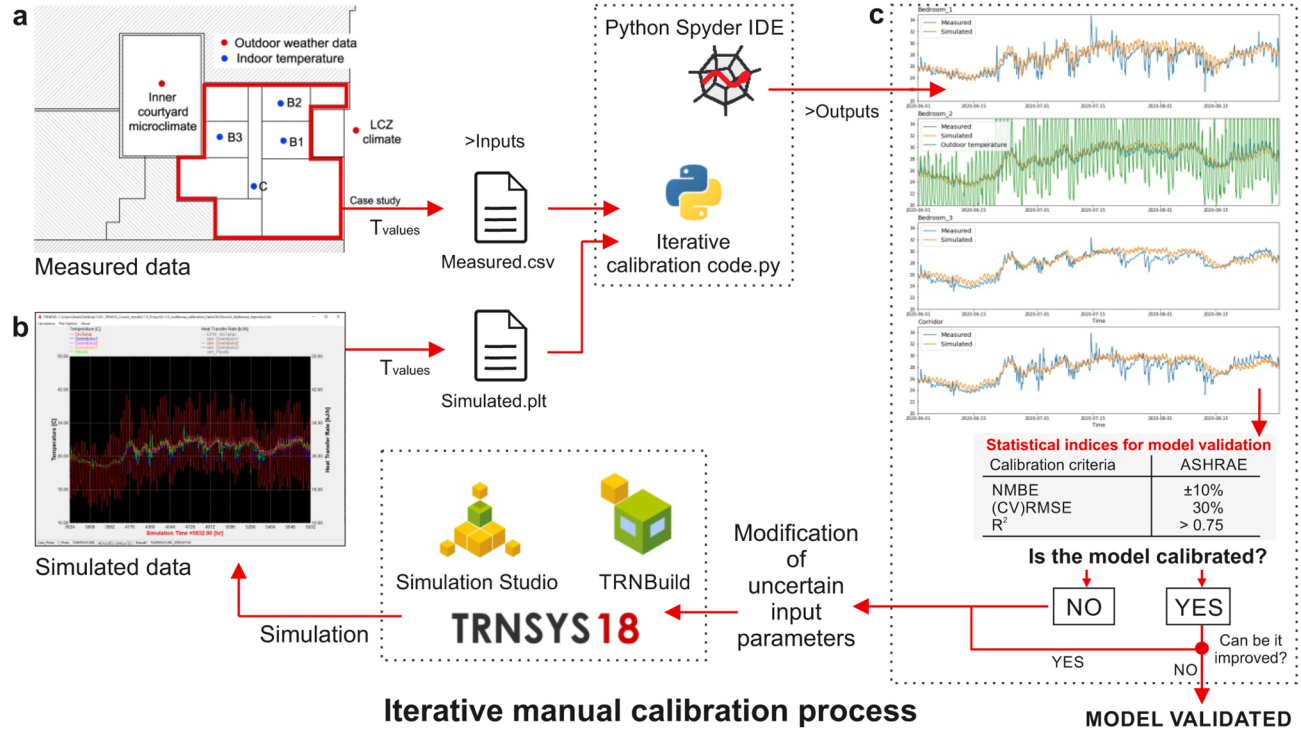


Figure 4. Iterative manual calibration workflow for model validation. a, Dwelling floor plan indicating measured data used for model calibration and validation. b, TRNSYS visualisation of simulated temperature profiles. c, Results of python script after each simulation interaction, providing the statistical indices to verify the model accuracy and validate the model.

The air temperature data of four indoor rooms in the dwelling were used to calibrate and validate the model since the main target of the manuscript is focused on building performance concerning indoor temperature oscillation. Measured rooms are indicated in Fig. 4a: bedroom1 (B1), bedroom2 (B2), bedroom3 (B3) and corridor (C). Data loggers (model TESTO 174H) were used to measure indoor air temperature. Sensors were installed at least 0.5 m away from the wall and at least 1.5 m away from windows. The logging interval was defined every 15 minutes. Then, the time series frequency was resampled to obtain mean air temperature values every hour for model calibration. The measured data were iteratively compared with the simulated values obtained from TRNSYS following the workflow defined in Fig. 4, in which statistical indices were automatically calculated after each simulation (Coakley et al., 2014). With this process, uncertain input parameters of the existing building, mainly related to thermal transmittance, infiltration rate, natural ventilation, heat flow schedules of internal gains and other operating conditions (such as air coupling or shading factors), were iteratively modified within the estimated

ranges until the simulated data converged with the measured data sets. The final parametrisation values were those reported in section 3.2.

The standard statistical indices used for model validation were the Normalized Mean Bias Error (NMBE), the Coefficient of Variation of the Root Mean Square Error (CV-RMSE) and the Coefficient of determination ( $R^2$ ), whose final results are shown in Table 2. The validated model fulfils the ASHRAE Guideline, which recommends that for good hourly reliability, the simulation model should have an NMBE lower than  $\pm 10\%$  and a CV-RMSE lower than 30%. Additionally, a minimum  $R^2$  value of 0.75 is recommended (*ASHRAE Handbook - Fundamentals*, 2017; Ruiz & Bandera, 2017).

Table 2: Statistical indices for model validation following ASHRAE Guideline 14-2014.

	NMBE	CV-RMSE	$R^2$
Bedroom1 (B1)	-2.0% ( $< \pm 10\%$ )	3.9% ( $< 30\%$ )	0.77 ( $> 0.75$ )
Bedroom2 (B2)	-0.5% ( $< \pm 10\%$ )	2.0% ( $< 30\%$ )	0.93 ( $> 0.75$ )
Bedroom3 (B3)	-1.5% ( $< \pm 10\%$ )	3.0% ( $< 30\%$ )	0.84 ( $> 0.75$ )
Corridor (C)	-1.2% ( $< \pm 10\%$ )	3.5% ( $< 30\%$ )	0.76 ( $> 0.75$ )

### 3.5. Building performance indicators

The building performance in different urban climate and microclimate scenarios was evaluated through the following indicators: percentage of indoor discomfort hours (DH, %) in free-running conditions and cooling energy demand (kWh/m<sup>2</sup>) using an idealised cooling system.

The percentage of indoor discomfort hours (DH, %) was evaluated simulating the building in free-running conditions (without AC systems) following the adaptive thermal comfort model defined in (*EN 16798-1*, 2019). This model describes the range of acceptable operative air temperature levels depending on the outdoor temperature. Indoor operative temperature per scenario was calculated as a weighted mean value for each room area. Then, the discomfort period was obtained per each comfort category (I, II and III), which defines the acceptability limit of indoor operative temperature. Category I corresponds to the high level of expectation and it is recommended for spaces occupied by very sensitive and fragile persons; category II is for a normal level of

expectation, mainly used for new buildings and renovations; and category III for an acceptable, moderate level of expectation, mainly for existing buildings. The limit values of each category are obtained through linear correlations defined in Eq. 2, based on the running mean outdoor air temperature ( $\Theta_{rm}$ , °C) ranging between 10 °C and 30 °C (see limits in Fig. 8).

$$\begin{aligned}
 \text{Upper limit of Category III (°C)} &= 0.33 \cdot \Theta_{rm} + 18.8 + 4 \\
 \text{Upper limit of Category II (°C)} &= 0.33 \cdot \Theta_{rm} + 18.8 + 3 \\
 \text{Upper limit of Category I (°C)} &= 0.33 \cdot \Theta_{rm} + 18.8 + 2 \\
 \text{Lower limit of Category I (°C)} &= 0.33 \cdot \Theta_{rm} + 18.8 - 3 \\
 \text{Lower limit of Category II (°C)} &= 0.33 \cdot \Theta_{rm} + 18.8 - 4 \\
 \text{Lower limit of Category III (°C)} &= 0.33 \cdot \Theta_{rm} + 18.8 - 5
 \end{aligned} \tag{2}$$

Running mean outdoor air temperature ( $\Theta_{rm}$ , °C) per day was calculated according to Eq. 3. This free-running condition is commonly found in residential buildings in the Mediterranean climate, where AC systems, predominantly located in some single rooms within the dwellings, are used sporadically when necessary (Domínguez-Amarillo et al., 2020; Lizana et al., 2016; Sendra et al., 2013).

$$\begin{aligned}
 \Theta_{rm(ed)} = & (\Theta_{ed-1} + 0.8 \cdot \Theta_{ed-2} + 0.6 \cdot \Theta_{ed-3} + 0.5 \cdot \Theta_{ed-4} + 0.4 \cdot \Theta_{ed-5} \\
 & + 0.3 \cdot \Theta_{ed-6} + 0.2 \cdot \Theta_{ed-7}) / 3.8
 \end{aligned} \tag{3}$$

where:

$\Theta_{rm(ed)}$ : mean outdoor air temperature of focus day.

$\Theta_{ed-n}$ : daily mean outdoor air temperature for n-days prior to focus day.

The cooling energy demand (kWh/m<sup>2</sup>) per scenario was evaluated considering an idealised cooling condition with two cooling set-point temperatures in whole indoor dwelling spaces, taking as reference the values recommended by the National EPC procedure (IDAE, 2009) and (EN 16798-1, 2019): 27°C at night and 25°C throughout the day. This indicator is different from the electricity consumption required to meet the cooling demand, as this last value will be dependent on the type and efficiency of the system used. A sensitivity analysis considering different cooling energy consumption patterns was also developed. Three cooling-related occupant

behaviour patterns were evaluated according to low, medium and high energy consumption profiles (Serrano-Jiménez et al., 2019). Low consumption is associated with an intermittent cooling pattern of 4 hours per day. Medium consumption is related to the standard EPC procedure profile (15 hours per day). A high consumption pattern means continuous cooling throughout the day (24 hours per day with cooling on). All the results are correlated to the conditioned floor area to facilitate comparison with other studies (kWh/m<sup>2</sup>) (Lizana et al., 2018).

## **4. Results and discussions**

The potential benefits of courtyard microclimate to mitigate extreme heat effects in buildings are analysed and discussed in three steps. Firstly, the measured weather datasets related to different urban climates and microclimates are compared. Secondly, the building performance is analysed under free-running conditions and with the operation of AC systems, comparing the percentage of indoor discomfort hours and cooling energy needs for each scenario. Finally, a sensitivity analysis is used to assess the potential benefits of inner courtyards as a climate-resilient building configuration, highlighting the most influential parameters to take advantage of these microclimates.

### **4.1. Evaluation of different urban climates and microclimates.**

The weather datasets collected from different urban climates and microclimates from 01st June 2020 to 31st August 2020 are compared in Fig. 5. This shows the full distribution of the outdoor air temperature data per dataset, with three horizontal lines indicating the median, maximum and minimum values. The datasets are associated with the specific microclimate of the courtyard at 4.5 and 15.0 m above the courtyard floor, the urban climate in the measured LCZ, the rural conditions of the Seville weather station and the TY weather file.

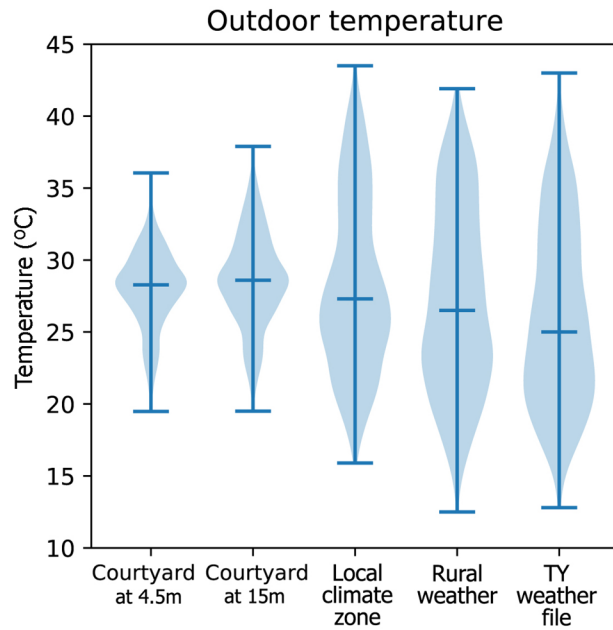


Figure 5. Violin plot of weather datasets. The area filled in represents the data distribution. Horizontal lines indicate the median, maximum and minimum values.

The data comparison shows how the urban climate associated with the LCZ presents higher temperature values than rural weather and the TY weather file. Moreover, the thermal buffer effect of the courtyard microclimate is highlighted at 4.5 m and 15.0 m, decreasing peak temperatures. This reduced thermal oscillation inside the courtyard is mainly produced due to the specific flow patterns inside the courtyard, characterised by low air change rates, and the thermal inertia of courtyard walls, which receive less solar radiation, mitigating peak temperature conditions (Zamani et al., 2018). Fig. 6 illustrates the evolution of maximum and minimum daily outdoor air temperatures, which introduces a better understanding of the behaviour of each weather dataset.

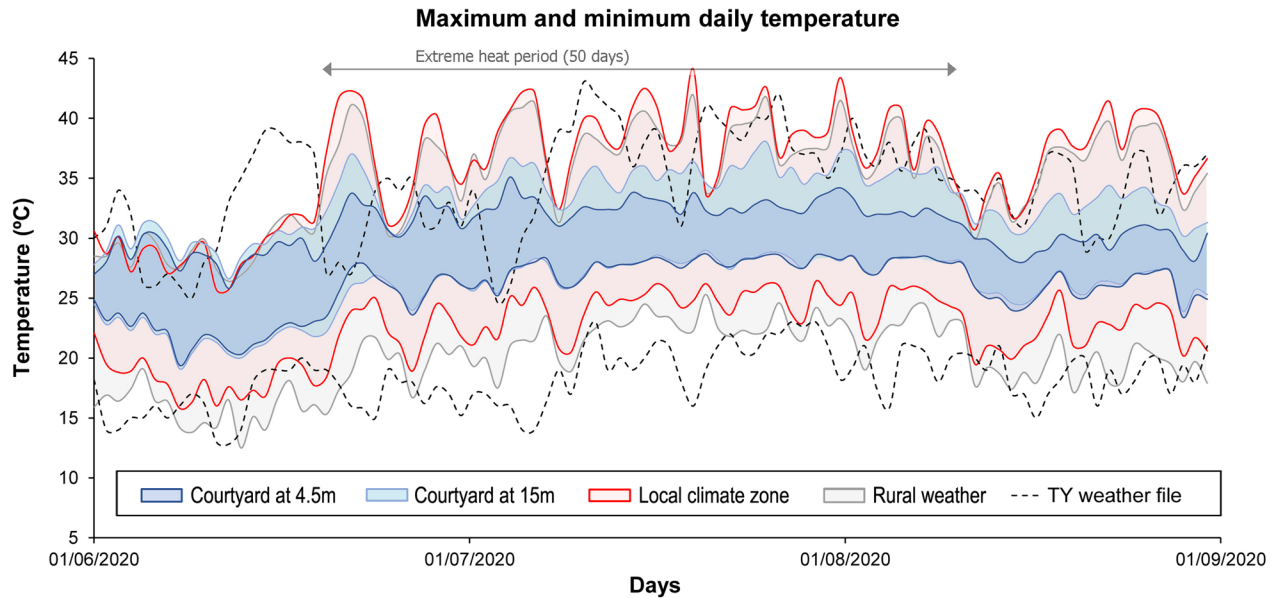


Figure 6. The maximum and minimum daily outdoor air temperature of different urban climates and microclimates throughout the summer season.

Urban overheating increases maximum daytime temperatures by a mean value of 0.8°C and above 1.5°C for peak days. Moreover, minimum night temperatures are increased by a mean value of 2.5°C during the measured period, with some peak overheating days above 6°C.

The data collected also show the thermal benefits of the inner courtyard microclimate in comparison with the LCZ. The courtyard was able to mitigate daily maximum air temperature by a mean value of 2.9 °C and 5.1°C at 15.0 m and 4.5m, respectively. Moreover, during extreme heatwave periods, with maximum outdoor temperatures above 41.2°C, the courtyard was able to reduce peak temperatures by up to 7.7°C and 12.4°C at 15.0 m and 4.5 m, respectively. The greater the heat impact, the higher the thermal benefits of the courtyard microclimate. Additionally, it can be observed that the minimum temperatures inside the courtyard at night are higher than the urban climate. This is due to the specific flow patterns inside the courtyard, characterised by low air change rates and the thermal inertia of courtyard walls, which can negatively or positively impact building performance according to the indoor ventilation pattern. In the case of single-sided ventilation of an indoor space to the courtyard, these conditions can negatively affect the indoor environment at night. However, in the case of

cross ventilation, this higher temperature will produce a stack effect that favours natural and cross ventilation through indoor spaces, increasing the air change rates for night-time free cooling.

Additionally, it should also be noted how the TY weather file for this region shows lower air temperatures during the entire summer period (Figs. 5 and 6). In fact, minimum temperatures are much lower than those measured in the rural area, not reflecting the data registered for this period (Fig. 6).

## **4.2. Impact of urban climates and microclimates on building performance**

The impact of different weather datasets on building performance was evaluated through two conditions. The calibrated building model simulated under free-running conditions per scenario (without any AC system) is analysed and discussed in section 4.2.1, evaluating the indoor discomfort hours through the adaptive comfort model per scenario. Afterwards, the building model simulated with an idealised cooling condition per scenario is analysed and discussed in section 4.2.2, evaluating the cooling energy needs per scenario.

### **4.2.1. Building scenarios under free-running conditions**

The distribution of the indoor air temperature per building scenario in free-running conditions is represented in Fig. 7. S2, related to urban climate in the specific LCZ, presents the highest indoor temperature distribution. In contrast, S1 and S3, associated with the courtyard microclimate and rural climate, show similar indoor temperature data distribution. This parallel performance between S1 and S3 highlights the potential heat mitigation effect of courtyard microclimate at 15.0m, which results in a similar behaviour of the S1 building model to that simply considering the rural weather dataset without the urban overheating effect. The mitigation of maximum peak temperatures by the courtyard microclimate in S1 provides a positive impact on indoor space, reducing heat gains by transmission, infiltration and ventilation during daytime. Additionally, the results in S4, associated with the TY weather file and taken as a reference value, show the lowest maximum, minimum and median values in comparison with other scenarios.

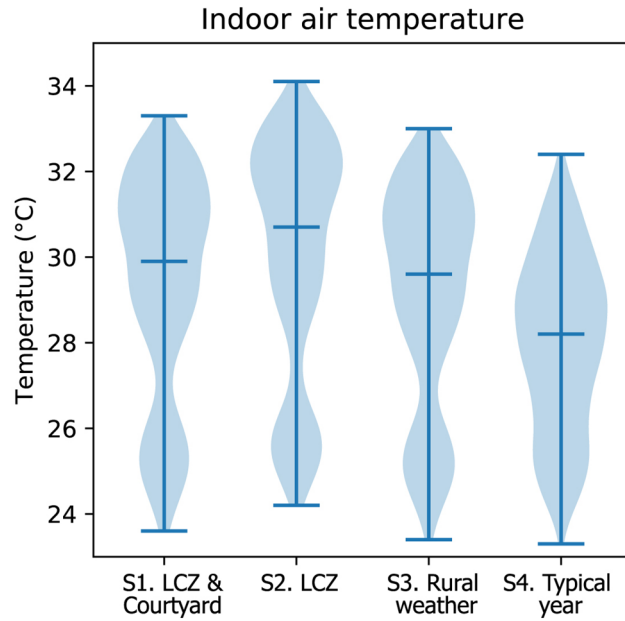


Figure 7. Violin plot of indoor air temperature per scenario simulated. The area filled in represents the data distribution and the three horizontal lines indicate the median, maximum and minimum values.

The impact of different urban climate and microclimate scenarios on building performance was evaluated from the point of view of comfort in Fig 8. This figure illustrates the indoor operative temperature oscillation (Top, °C) in relation to running mean external temperature ( $\Theta_{rm}$ , °C) for all simulated scenarios according to the European adaptive comfort model (EN 16798-1, 2019).



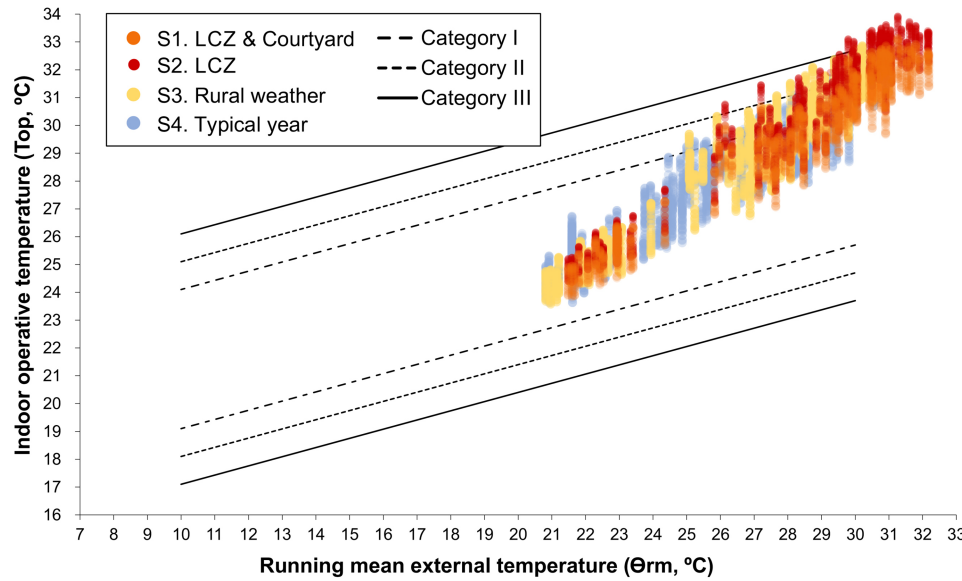


Figure 8. Adaptive comfort model of dwelling performance per individual scenario, based on EN 16798-1:2019.

The results show how the indoor operative air temperature values obtained in S1 (orange) are lower than those in S2 (red). These lower temperatures are associated with the benefit of courtyard microclimate in S1, which can mitigate extreme heat impact in the building analysed in S2. The results highlight how considering two outdoor weather conditions affecting the building has a considerable benefit in final building performance. S3 (yellow), relating to the building affected by rural weather data, provides even lower indoor operative temperature periods than S1. In this case, the building model was simulated using just one outdoor weather condition related to rural weather, neglecting the impact of urban overheating, which considerably increases the comfort period. Finally, S4, associated with the building model simulated using the TY weather file, results in much lower indoor operative temperatures. These results show how TY weather files cannot effectively reflect the building performance under extreme heat climate events. Thus, these files help predict long-term energy-related performance but would not be suitable for supporting a climate-resilient building design.

Fig. 9 quantifies the differences from the comfort point of view between the building scenarios in different outdoor climates and microclimates. It shows the percentage of indoor discomfort hours per comfort category according

to the European adaptive comfort model (EN 16798-1, 2019), involving the entire period measured from June to August (Fig. 9a) and the extreme heat period alone (see Fig. 6) from 20<sup>th</sup> June to 10<sup>th</sup> August (Fig. 9b).

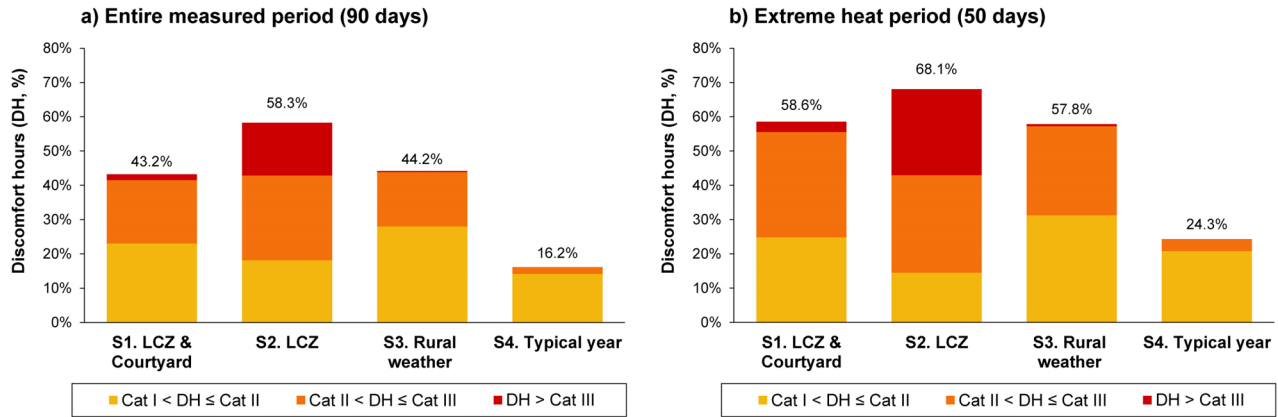


Figure 9. Percentage of indoor discomfort hours (DH) per comfort category according to the adaptive comfort model defined by EN 16798-1:2019. a, Discomfort hours calculated throughout the entire measured period, from 01<sup>st</sup> June 2020 to 31<sup>st</sup> August 2020. b, Discomfort hours calculated throughout the extreme heat period measured from 20<sup>th</sup> June 2020 to 10<sup>th</sup> August 2020 (see Fig. 6).

The results clearly demonstrate the thermal benefits of courtyard microclimate for mitigating heat impact on buildings. A comparison of S1 and S2 shows how the courtyard was able to reduce indoor discomfort hours by 26% (from 58.3% to 43.2%) during the entire measured period (Fig. 9a), and by 14% (from 68.1% to 58.6%) throughout the extreme heat period (Fig. 9b). Moreover, severe discomfort hours, associated with discomfort hours higher than category III, were almost eliminated, with a reduction of up to 88% for both timeframes. Furthermore, the comparison of S1 and S3 demonstrates how the thermal response of the building involving the courtyard benefits is very similar to the building performance with rural weather data, without considering the urban overheating effects. This means that the courtyard was able to mitigate almost all the building overheating produced by the urban climate in scenario 2. Finally, S4 shows a percentage of DH of 16.2% and 24.3%, respectively, much lower than other scenarios. These values should be taken as a reference value but also manifest the unsuitability of TY weather files for supporting a climate-resilient building design to face extreme heat periods.

#### 4.2.2. Building scenarios under idealised cooling conditions

Regarding cooling energy balance, Fig. 10 compares the cooling energy demand for each building scenario in kWh/m<sup>2</sup>. Error bars show the maximum and minimum values obtained through sensitivity analysis using low, medium, and high cooling-related occupant behaviour patterns.

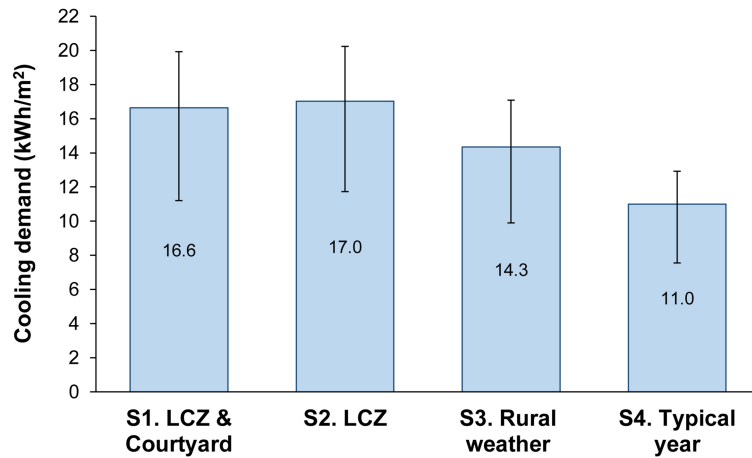


Figure 10. Cooling energy demand per scenario calculated throughout the entire measured period, from 01st June 2020 to 31st August 2020.

The results highlight how the impact of extreme weather conditions and the urban climate in cooling energy demand in S2 is considerable compared to rural (S3) and TY weather scenarios (S4). The urban climate in the LCZ (S2) increases cooling needs by 2.7 kWh/m<sup>2</sup> (19%) compared to rural conditions and by 6.0 kWh/m<sup>2</sup> (55%) compared to TY weather data (S4). Similar to the comparison of scenarios in free-running conditions, the results show how TY weather files cannot effectively reflect the overheating building performance in the urban climate. In this situation with AC systems, the courtyard (S1) was able to mitigate the increased cooling needs due to urban overheating by 15% (0.4 kWh/m<sup>2</sup> of 2.7 kWh/m<sup>2</sup>), and by up to 29% (0.52 kWh/m<sup>2</sup> of 1.8 kWh/m<sup>2</sup>) in the situation with a low energy consumption pattern (lower error bar value). The more sporadic or intermittent the use of the conditioning systems, the greater the thermal benefit obtained by the courtyard microclimate.

### 4.3. Optimal climate-resilient building configuration using the courtyard microclimate.

The thermal benefits of courtyard microclimate in building performance differ during the day and night. During the day, the courtyard reduces maximum peak outdoor air temperatures, as illustrated in Fig. 11a, decreasing the transmission and infiltration thermal losses of the building façade facing the inner courtyard. In addition, the courtyard geometry reduces the solar gains of the rooms in this area. On the other hand, during the night, the courtyard temperature is higher than the urban climate, producing a stack effect that favours natural and cross ventilation through indoor spaces, increasing the air change rates for night-time free cooling (Fig. 11b).

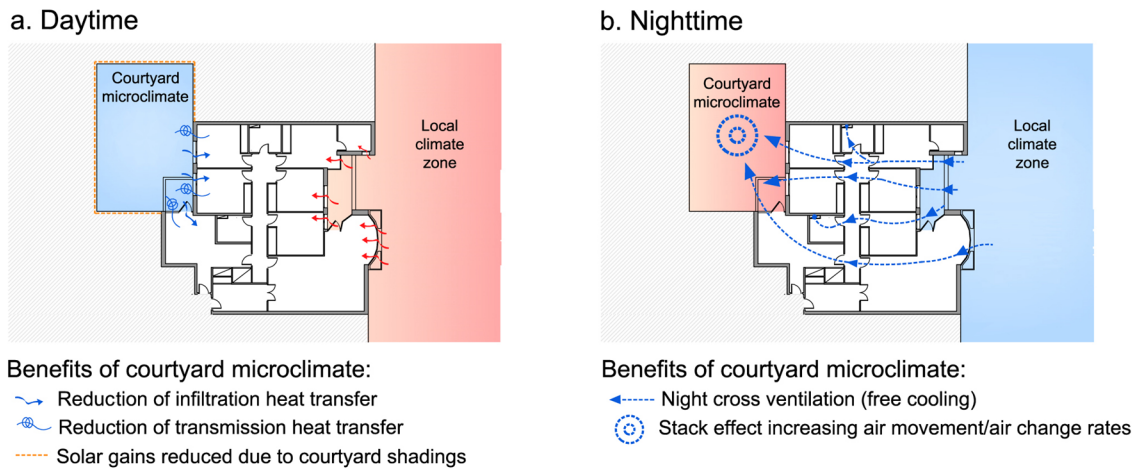


Figure 11. Schematic diagram of bioclimatic strategy to enhance building performance using courtyard microclimate.

Fig. 12 shows a sensitivity analysis of the most influential parameters in building performance in free-running conditions (Fig. 12a) and with idealised cooling conditions (12b). It evaluates the input data variation by  $\pm 50\%$ , associated with infiltration leakage rate (ACH of  $0.6 \text{ h}^{-1}$ ), night ventilation rate due to windows openings and façade U-value ( $0.74 \text{ W/m}^2 \text{ K}$ ), previously defined in sections 3.1 and 3.2.

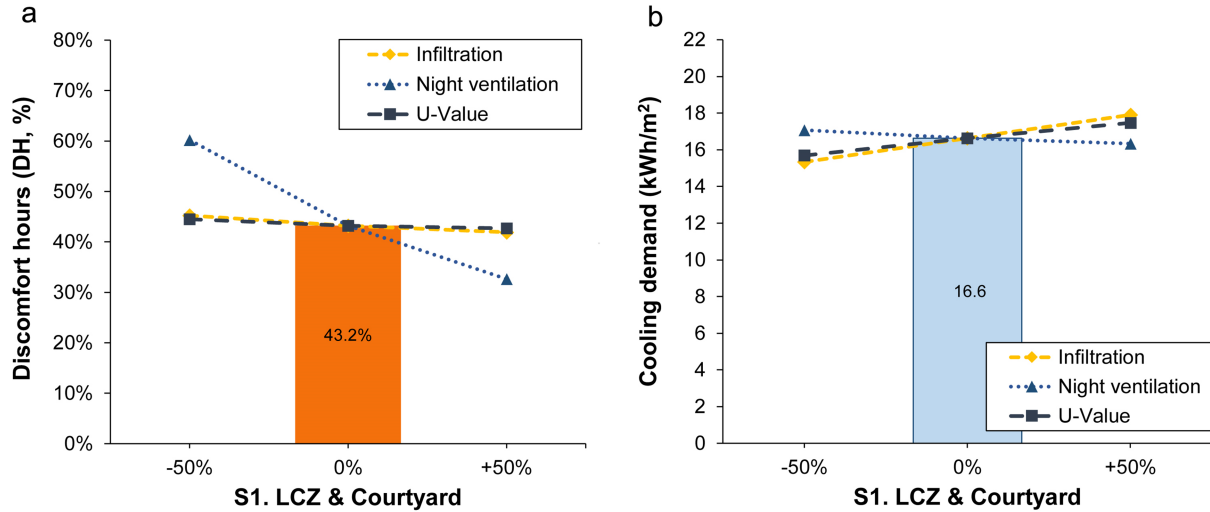


Figure 12. Sensitivity analysis of infiltration, night ventilation and façade U-value for scenario 1 (S1. Courtyard & LCZ). **a**, Percentage of indoor discomfort hours higher than Category I following the adaptive comfort model defined by EN 16798-1:2019 throughout the entire measured period, from 01st June 2020 to 31st August 2020. **b**, Cooling energy demand calculated throughout the entire measured period.

Night ventilation has a similar influence in both simulated conditions. An increase in night-time free-cooling decreases the indoor discomfort hours in free-running conditions (dotted blue line in Fig. 12a) and the cooling demand in the case of having AC systems (dotted blue line in Fig. 12b). However, the effect is most limited using the cooling energy demand indicator (Fig. 12b) since night-time outdoor temperature in urban climate is higher due to the UHI impact, which remains above the cooling set-point most of the time. In contrast, infiltration and façade U-value display the opposite performance when comparing free-running conditions (Fig. 12a) and idealised cooling conditions (Fig. 12b). From the point of view of cooling energy demand, the lower the infiltration rate or U-value, the lower the cooling demand. This is the reason why all building standards follow these criteria as a guideline to improve building energy efficiency. However, in the case of indoor discomfort hours in free-running conditions without any AC system, a decrease of these parameters worsens the building performance, hindering the release of heat gains absorbed. Similar statements are found in (Toparlar et al., 2018). This situation, often found in energy poverty situations, makes the passive strategy of the courtyard microclimate a promising alternative in comparison with conventional energy conservation measures, as is further demonstrated below.

Fig. 13 shows a sensitivity analysis of the impact of courtyard microclimate on building performance in free-running conditions (Fig. 13a) and with idealised cooling conditions (Fig. 13b). The building model simulated with the courtyard temperature oscillation at 15.0 m above the courtyard floor, as illustrated in Fig. 2, represents the conditions previously reported for S1. Using this reference case, the courtyard climate node was modified by considering the courtyard temperature found at 4.5 m above the floor (previously shown in Figs. 5 and 6), and without considering the courtyard benefit (S2).

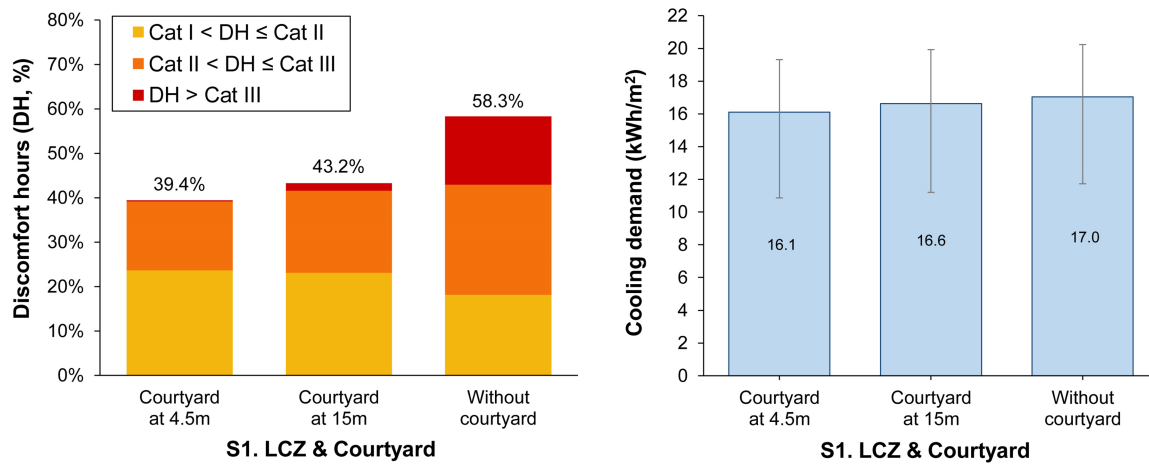


Figure 13. Sensitivity analysis of courtyard microclimate for scenario 1 (S1. Courtyard & LCZ). **a**, Percentage of indoor discomfort hours per comfort category following the adaptive comfort model defined by EN 16798-1:2019 throughout the entire measured period, from 01st June 2020 to 31st August 2020. **b**, Cooling energy demand calculated throughout all measured period.

The results demonstrate how enhancing the courtyard microclimate, in this case using the data collected at 4.5m, it is possible to improve the building performance for both situations, with and without the operation of AC systems. This means that implementing different strategies to improve the courtyard microclimate can act as a potential passive cooling strategy to reduce the indoor discomfort hours and the cooling energy demand in the building. These strategies can include adding additional shading devices to reduce solar gains inside the courtyard, vegetation or modifying the courtyard aspect ratio (Galán-Marín et al., 2018; Lopez-Cabeza et al., 2020; Victoria Patricia López-Cabeza et al., 2018).

While S1 was able to reduce indoor discomfort hours by 26% (courtyard at 15.0 m), the enhanced courtyard situation (courtyard temperature oscillation at 4.5m) was able to reduce the discomfort period by up to 32%, even

improving on the building comfort conditions found in S3, associated with the rural weather scenario. Moreover, in the case of cooling demand, the enhanced courtyard situation was able to mitigate the increase in cooling energy demand due to the urban climate from 15% (0.4 kWh/m<sup>2</sup> of 2.7 kWh/m<sup>2</sup>) to 34% (0.9 kWh/m<sup>2</sup> of 2.7 kWh/m<sup>2</sup>), and by up to 47% (0.9 kWh/m<sup>2</sup> of 1.8 kWh/m<sup>2</sup>) in the case of a low energy consumption pattern (lower error bar value).

This paper introduces for the first time a complete building performance simulation using multi-nodal outdoor conditions to take into consideration the potential benefits of urban microclimates. The results demonstrate and quantify how considering multi-nodal outdoor conditions can enable additional passive cooling strategies to mitigate climate risks in the urban context, improving buildings' comfort and well-being. However, further studies are required in different locations, urban morphologies and microclimates to thoroughly validate the extended use of this approach for building modelling in future regulations.

## **5. Conclusions**

This research evaluates the impact of different urban climates on building performance and demonstrates the benefits of specific microclimate conditions, such as inner courtyards, to mitigate the effects of extreme heat events in buildings. A reference case study with an inner courtyard was numerically modelled with two outdoor weather nodes, the courtyard microclimate and the urban climate. The building model was iteratively calibrated and validated in TRNSYS using measured data. The building model scenario was then compared with three scenarios based on a single outdoor weather node: the local urban climate, rural weather data and a typical year weather file. Based on the results, the following conclusions were drawn:

From the point of view of weather data, the results show how urban climate increases indoor discomfort hours by 32% (from 44.2% to 58.3%) in free-running conditions and extend cooling energy demand by 19% (from 14.3 kWh/m<sup>2</sup> to 17.0 kWh/m<sup>2</sup>) in comparison with a rural weather scenario not affected by the urban overheating. Moreover, the results also show the unsuitability of typical year weather files to evaluate the climate resilience of

buildings and cities. Overheating events in cities, which will happen more often in the future and will be worsened by the urban overheating phenomenon, require the consideration of these extreme urban weather conditions in order to support an efficient climate-resilient building design.

Regarding building performance indicators, it is observed that although energy conservation and efficiency measures are effective actions for improving building performance through metrics relating to cooling energy demand and associated impacts, they can increase the building discomfort period in free-running conditions. The highly insulated buildings or airtightness can hinder the release of absorbed heat gains if ventilation is not adequately addressed, increasing overheating. This scenario, which often affects people in energy poverty, highlights the inefficiency of current directives for supporting a climate-resilient building design in cities. Existing policies should move beyond energy efficiency targets towards a climate-resilient pathway implementing new comfort indicators based on free-running conditions.

Finally, the results demonstrate how building simulation with multi-nodal outdoor conditions can enable additional passive cooling alternatives based on specific urban microclimates to mitigate climate risks in buildings. Moreover, the results highlight courtyard microclimate as a powerful strategy for tackling extreme heat periods from the point of view of comfort and cooling energy demand in buildings. The courtyard microclimate can completely mitigate the impact of extreme heat in free-running conditions, eliminating severe indoor discomfort hours by over 88%. Moreover, it can reduce the increase in cooling energy demand due to the urban climate by 15% (0.4 kWh/m<sup>2</sup> of 2.7 kWh/m<sup>2</sup>) and by up to 34% (0.9 kWh/m<sup>2</sup> of 2.7 kWh/m<sup>2</sup>) by following specific strategies to enhance the courtyard thermal buffer. The reduction in daytime peak outdoor temperature, the stack effect increasing natural and cross ventilation at night, and the courtyard shadings provide huge passive cooling benefits that protect the building against extreme heat conditions.



Future studies in different locations, urban morphologies and microclimates should be promoted to thoroughly validate the extended use of this multi-nodal outdoor simulation approach in future building regulations to enable additional strategies based on urban microclimates to mitigate climate change impacts in buildings and cities.

## **Acknowledgements**

This work was supported by the National Government of Spain, Ministerio de Ciencia, Innovación y Universidades through the research project RTI2018-093521-B-C33 and a Juan de la Cierva Postdoctoral Fellowship granted to J. Lizana (FJC2019-039480-I); and the Spanish Ministry of Education, Culture and Sport via two pre-doctoral contracts granted to V.P. L-C. (FPU17/05036) and E. D-M (FPU18/04783). The research was also supported by the European Union's Horizon 2020 research and innovation programme under the Marie Skłodowska-Curie grant agreement No 101023241. Moreover, the authors would also like to thank AEMET (State Meteorological Agency of Spain) for the weather data provided to carry out this research.

## References

- AEMET. (2019). *Olas de calor en España desde 1975*. Área de Climatología y Aplicaciones Operativas (AEMET). [http://www.aemet.es/es/conocermas/recursos\\_en\\_linea/publicaciones\\_y\\_estudios/estudios/detalles/olascalor](http://www.aemet.es/es/conocermas/recursos_en_linea/publicaciones_y_estudios/estudios/detalles/olascalor)
- AEMET. (2020). *Listado de provincias afectadas por las Olas de calor registradas desde 1975*. [http://www.aemet.es/es/conocermas/recursos\\_en\\_linea/publicaciones\\_y\\_estudios/estudios/detalles/olascalor](http://www.aemet.es/es/conocermas/recursos_en_linea/publicaciones_y_estudios/estudios/detalles/olascalor)
- Altunkasa, C., & Uslu, C. (2020). Use of outdoor microclimate simulation maps for a planting design to improve thermal comfort. *Sustainable Cities and Society*, 57(March), 102137. <https://doi.org/10.1016/j.scs.2020.102137>
- ASHRAE. (2014). *ASHRAE Guideline 14-2014. Measurement of Energy, Demand, and Water Savings*. American Society of Heating, Ventilating, and Air Conditioning Engineers (ASHRAE). [www.ashrae.org/technology](http://www.ashrae.org/technology).
- ASHRAE Handbook - Fundamentals* (SI Edition). (2017).
- Bardhan, R., Debnath, R., Gama, J., & Vijay, U. (2020). REST framework: A modelling approach towards cooling energy stress mitigation plans for future cities in warming Global South. *Sustainable Cities and Society*, 61(January), 102315. <https://doi.org/10.1016/j.scs.2020.102315>
- Bienvenido-Huertas, D., Sánchez-García, D., & Rubio-Bellido, C. (2020). Analysing natural ventilation to reduce the cooling energy consumption and the fuel poverty of social dwellings in coastal zones. *Applied Energy*, 279(September). <https://doi.org/10.1016/j.apenergy.2020.115845>
- Chan, A. L. S. (2011). Developing a modified typical meteorological year weather file for Hong Kong taking into account the urban heat island effect. *Building and Environment*, 46(12), 2434–2441. <https://doi.org/10.1016/j.buildenv.2011.04.038>
- Chen, D., & Chen, H. W. (2013). Using the Köppen classification to quantify climate variation and change: An example for 1901–2010. *Environmental Development*, 6(1), 69–79. <https://doi.org/10.1016/j.envdev.2013.03.007>
- Chi, F., Xu, L., & Peng, C. (2020). Integration of completely passive cooling and heating systems with daylighting function into courtyard building towards energy saving. *Applied Energy*, 266(January), 114865. <https://doi.org/10.1016/j.apenergy.2020.114865>
- CIBSE. (2007). *Guide A: Environmental design*.
- Coakley, D., Raftery, P., & Keane, M. (2014). A review of methods to match building energy simulation models to measured data. *Renewable and Sustainable Energy Reviews*, 37, 123–141. <https://doi.org/10.1016/j.rser.2014.05.007>
- Crawley, D. B., Lawrie, L. K., & Systems, B. (2019). Should We Be Using Just ‘Typical’ Weather Data in Building Performance Simulation? *16th International Building Performance Simulation Association (IBPSA) Conference*, 2–4. <https://doi.org/10.26868/25222708.2019.210594>
- Cui, Y., Yan, D., Hong, T., Xiao, C., Luo, X., & Zhang, Q. (2017). Comparison of typical year and multiyear building simulations using a 55-year actual weather data set from China. *Applied Energy*, 195, 890–904. <https://doi.org/10.1016/j.apenergy.2017.03.113>
- De Gids, W., & Phaff, H. (1982). Ventilation rates and energy consumption due to open windows: A brief overview of

research in the Netherlands. *Air Infiltration Review*, 4(1), 4–5.

- Diz-Mellado, E., López-Cabeza, V. P., Rivera-Gómez, C., Galán-Marín, C., Rojas-Fernández, J., & Nikolopoulou, M. (2021). Extending the adaptive thermal comfort models for courtyards. *Building and Environment*, 203(June). <https://doi.org/10.1016/j.buildenv.2021.108094>
- Diz-Mellado, E., Rubino, S., Fernández-García, S., Gómez-Mármol, M., Rivera-Gómez, C., & Galán-Marín, C. (2021). Applied machine learning algorithms for courtyards thermal patterns accurate prediction. *Mathematics*, 9(10), 1–19. <https://doi.org/10.3390/math9101142>
- Domínguez-Amarillo, S., Fernández-Agüera, J., Peacock, A., & Acosta, I. (2020). Energy related practices in Mediterranean low-income housing. *Building Research and Information*, 48(1), 34–52. <https://doi.org/10.1080/09613218.2019.1661764>
- EEA. (2019). *The European Environment: State and Outlook 2020. Knowledge for transition to a sustainable Europe*. European Environment Agency.
- EN 13465:2004. Ventilation for buildings. Calculation methods for the determination of air flow rates in dwellings., (2004).
- EN 15193-1:2017. Energy performance of buildings. Energy requirements for lighting. Part 1: Specifications, Module M9, (2017).
- EN 15242. (2007). *EN 15242:2007. Ventilation for buildings. Calculation methods for the determination of air flow rates in buildings including infiltration*.
- EN 16798-1:2019. *Energy performance of buildings. Ventilation for buildings. Part 1: Indoor environmental input parameters for design and assessment of energy performance of buildings addressing indoor air quality, thermal environment, lighting and acoust.* (2019).
- EN 16798-2:2019. *Energy performance of buildings - Ventilation for buildings - Part 2: Interpretation of the requirements in EN 16798-1 - Indoor environmental input parameters for design and assessment of energy performance of buildings addressing indoor.* (2019).
- EN 16798-7:2017. *Energy performance of buildings. Ventilation for buildings. Part 7: Calculation methods for the determination of air flow rates in buildings including infiltration (Modules M5-5)*. (2017).
- EnergyPlus. *Weather Data for simulations*. (n.d.). Retrieved October 30, 2020, from <https://energyplus.net/weather>
- Escandón, R., Suárez, R., & Sendra, J. J. (2017). On the assessment of the energy performance and environmental behaviour of social housing stock for the adjustment between simulated and measured data: The case of mild winters in the Mediterranean climate of southern Europe. *Energy and Buildings*, 152, 418–433. <https://doi.org/10.1016/j.enbuild.2017.07.063>
- Fabbri, K., & Costanzo, V. (2020). Drone-assisted infrared thermography for calibration of outdoor microclimate simulation models. *Sustainable Cities and Society*, 52(May 2019), 101855. <https://doi.org/10.1016/j.scs.2019.101855>
- Fabbri, Kristian, Gaspari, J., Bartoletti, S., & Antonini, E. (2020). Effect of facade reflectance on outdoor microclimate: An Italian case study. *Sustainable Cities and Society*, 54(July 2019), 101984. <https://doi.org/10.1016/j.scs.2019.101984>

- Fernández-Agüera, J., Domínguez-Amarillo, S., Sendra, J. J., & Suarez, R. (2019). Predictive models for airtightness in social housing in a Mediterranean region. *Sustainable Cities and Society*, 51(July), 101695. <https://doi.org/10.1016/j.scs.2019.101695>
- Fiorentini, M., Tartarini, F., Ledo Gomis, L., Daly, D., & Cooper, P. (2019). Development of an enthalpy-based index to assess climatic potential for ventilative cooling of buildings: An Australian example. *Applied Energy*, 251(April), 113169. <https://doi.org/10.1016/j.apenergy.2019.04.165>
- Forouzandeh, A. (2018). Numerical modeling validation for the microclimate thermal condition of semi-closed courtyard spaces between buildings. *Sustainable Cities and Society*, 36(August 2017), 327–345. <https://doi.org/10.1016/j.scs.2017.07.025>
- Galán-Marín, C., López-Cabeza, V. P., Rivera-Gómez, C., & Rojas-Fernández, J. M. (2018). On the Influence of Shade in Improving Thermal Comfort in Courtyards. *Proceedings*, 2(22), 1390. <https://doi.org/10.3390/proceedings2221390>
- Government of Spain. (2019). *AEMET State Meteorological Agency*. <http://www.aemet.es/>
- Hong, T., Ferrando, M., Luo, X., & Causone, F. (2020). Modeling and analysis of heat emissions from buildings to ambient air. *Applied Energy*, 277(April), 115566. <https://doi.org/10.1016/j.apenergy.2020.115566>
- Hothaps-Soft. *Climate Data and Heat Exposure Software*. (2014). <https://climatechip.org/hothaps-software>
- IDAE. (2009). *Condiciones de aceptación de Procedimientos alternativos a LIDER y CALENER*. Instituto para la Diversificación y Ahorro de la Energía (IDAE).
- IDAE. (2012). *Manual de fundamentos técnicos de calificación energética de edificios existentes CE3*. Instituto para la Diversificación y Ahorro de la Energía (IDAE).
- IEA. (2018). *The Future of Cooling. Opportunities for energy-efficient air conditioning*. IEA Publications. <https://www.iea.org/reports/the-future-of-cooling>
- IEA EBC Annex 62. (n.d.). *Ventilative Cooling*. 2018. <https://iea-ebc.org/projects/project?AnnexID=62>
- IEA EBC Annex 62. (2018). *Status and recommendations for better implementation of ventilative cooling in standards, legislation and compliance tools*. *Energy in Buildings and Communities Programme* (C. Plesner (Ed.)).
- INE. (2013). *Instituto Nacional de Estadística. Censo de Poblacion y Viviendas*.
- Instituto Nacional de Estadística. (2011). *Censos de Población y Vivienda*. [https://www.ine.es/censos2011\\_datos/cen11\\_datos\\_inicio.htm](https://www.ine.es/censos2011_datos/cen11_datos_inicio.htm)
- IPCC. (2014). *Climate Change 2014: Synthesis Report, Contribution of working Groups I, II and III to the Fifth Assessment Report of the Intergovernmental Panel on Climate Change*. IPCC. [https://doi.org/10.1016/S0022-0248\(00\)00575-3](https://doi.org/10.1016/S0022-0248(00)00575-3)
- ISO 13789:2017. Thermal performance of buildings - Transmission and ventilation heat transfer coefficients - Calculation method, (2017).
- ISO 52016-1:2017. Energy performance of buildings - Energy needs for heating and cooling, internal temperatures and sensible and latent heat loads - Part 1: Calculation procedures, (2017).
- ISO 7730:2005. *Ergonomics of the thermal environment. Analytical determination and interpretation of thermal comfort*

*using calculation of the PMV and PPD indices and local thermal comfort criteria.* (2005).

- Jiao, Z., Yuan, J., Farnham, C., & Emura, K. (2020). Deviation of design air-conditioning load based on weather database of reference weather year and actual weather year. *Energy and Built Environment*, 1(4), 417–422. <https://doi.org/10.1016/j.enbenv.2020.04.010>
- Johra, H., & Heiselberg, P. (2017). Influence of internal thermal mass on the indoor thermal dynamics and integration of phase change materials in furniture for building energy storage: A review. *Renewable and Sustainable Energy Reviews*, 69(September 2015), 19–32. <https://doi.org/10.1016/j.rser.2016.11.145>
- Kjellstrom, T., Gabrysch, S., Lemke, B., & Dear, K. (2009). The “hothaps” programme for assessing climate change impacts on occupational health and productivity: An invitation to carry out field studies. *Global Health Action*, 2(1), 2082. <https://doi.org/10.3402/gha.v2i0.2082>
- Köppen climate classification.* (n.d.). Retrieved February 22, 2021, from <http://hanschen.org/koppen>
- Larsen, T. S. (2006). *Natural Ventilation Driven by Wind and Temperature Difference*. Department of Civil Engineering, Aalborg University.
- Larsen, Tine S., & Heiselberg, P. (2008). Single-sided natural ventilation driven by wind pressure and temperature difference. *Energy and Buildings*, 40(6), 1031–1040. <https://doi.org/10.1016/j.enbuild.2006.07.012>
- Li, Y., Neill, Z. O., Zhang, L., Chen, J., Im, P., & Degraw, J. (2021). *Grey-box modeling and application for building energy simulations - A critical review.* 146(January).
- Lizana, J., Barrios-Padura, Á., Molina-Huelva, M., & Chacartegui, R. (2016). Multi-criteria assessment for the effective decision management in residential energy retrofitting. *Energy & Buildings*, 129, 284–307. <https://doi.org/10.1016/j.enbuild.2016.07.043>
- Lizana, J., de-Borja-Torrejon, M., Barrios-Padura, A., Auer, T., & Chacartegui, R. (2019). Passive cooling through phase change materials in buildings. A critical study of implementation alternatives. *Applied Energy*, 254, 113658. <https://doi.org/10.1016/j.apenergy.2019.113658>
- Lizana, J., Serrano-Jimenez, A., Ortiz, C., Becerra, J. A., & Chacartegui, R. (2018). Energy assessment method towards low-carbon energy schools. *Energy*, 159, 310–326. <https://doi.org/10.1016/j.energy.2018.06.147>
- Lopez-Cabeza, Galán-Marín, & Rivera-Gómez. (2020). Thermodynamic Performance Enhancement of Courtyards Using a Shading Device. *Proceedings*, 38(1), 17. <https://doi.org/10.3390/proceedings2019038017>
- López-Cabeza, V. P., Galán-Marín, C., Rivera-Gómez, C., & Roa-Fernández, J. (2018). Courtyard microclimate ENVI-met outputs deviation from the experimental data. *Building and Environment*, 144(August), 129–141. <https://doi.org/10.1016/j.buildenv.2018.08.013>
- López-Cabeza, V.P., Carmona-Molero, F. J., Rubino, S., Rivera-Gómez, C., Fernández-Nieto, E. D., Galán-Marín, C., & Chacón-Rebollo, T. (2021). Modelling of surface and inner wall temperatures in the analysis of courtyard thermal performances in Mediterranean climates. *Journal of Building Performance Simulation* ISSN:, 14(2), 181–202. <https://doi.org/10.1080/19401493.2020.1870561>

- López-Cabeza, Victoria Patricia, Galán-Marín, C., Rivera-Gómez, C., Roa-Fernández, J., & Borrego-Baena, J. M. (2018). Comparative Analysis of Thermal Performance between Courtyards in Mediterranean Climate. *Proceedings*, 2(22), 1381. <https://doi.org/10.3390/proceedings2221381>
- Mata, É., Wanemark, J., Nik, V. M., & Sasic, A. (2019). Economic feasibility of building retrofitting mitigation potentials : Climate change uncertainties for Swedish cities. *Applied Energy*, 242(August 2018), 1022–1035. <https://doi.org/10.1016/j.apenergy.2019.03.042>
- Natanian, J., Aleksandrowicz, O., & Auer, T. (2019). A parametric approach to optimizing urban form, energy balance and environmental quality: The case of Mediterranean districts. *Applied Energy*, 254(August). <https://doi.org/10.1016/j.apenergy.2019.113637>
- Natanian, J., & Auer, T. (2020). Beyond nearly zero energy urban design: A holistic microclimatic energy and environmental quality evaluation workflow. *Sustainable Cities and Society*, 56(February). <https://doi.org/10.1016/j.scs.2020.102094>
- NBE-CT-79. Norma Básica de la edificación sobre Condiciones Térmicas de los Edificios, (1979).
- Nik, V. M., & Arvidsson, J. (2017). Using Typical and Extreme Weather Files for Impact Assessment of Climate Change on Buildings. *Energy Procedia*, 132, 616–621. <https://doi.org/10.1016/j.egypro.2017.09.686>
- Perera, A. T. D., Coccolo, S., Scartezzini, J. L., & Mauree, D. (2018). Quantifying the impact of urban climate by extending the boundaries of urban energy system modeling. *Applied Energy*, 222(December 2017), 847–860. <https://doi.org/10.1016/j.apenergy.2018.04.004>
- Plesner, C., Larsen, T., & Leprince, V. (2016). Calculation methods for single-sided natural ventilation - simplified or detailed? *CLIMA 2016 - Proceedings of the 12th REHVA World Congress: Volume 5*.
- Ratti, C., Di Sabatino, S., & Britter, R. (2006). Urban texture analysis with image processing techniques: Winds and dispersion. *Theoretical and Applied Climatology*, 84(1–3), 77–90. <https://doi.org/10.1007/s00704-005-0146-z>
- Rivera-Gómez, C., Diz-Mellado, E., Galán Marín, C., & López Cabeza, V. (2019). Tempering potential-based evaluation of the courtyard microclimate as a combined function of aspect ratio and outdoor temperature. *Sustainable Cities and Society*, 51(August), 101740. <https://doi.org/10.1016/j.scs.2019.101740>
- Rojas-Fernández, J., Galán-Marín, C., Rivera-Gómez, C., & Fernández-Nieto, E. D. (2018). Exploring the interplay between CAD and FreeFem++ as an energy decision-making tool for architectural design. *Energies*, 11(10). <https://doi.org/10.3390/en1102665>
- Ruiz, G. R., & Bandera, C. F. (2017). Validation of calibrated energy models: Common errors. *Energies*, 10(10). <https://doi.org/10.3390/en10101587>
- Samuelson, H. W., Baniassadi, A., & Izaga Gonzalez, P. (2020). Beyond energy savings: Investigating the co-benefits of heat resilient architecture. *Energy*, 204, 117886. <https://doi.org/10.1016/j.energy.2020.117886>
- Sánchez de la Flor, F. J., Ruiz-Pardo, Á., Diz-Mellado, E., Rivera-Gómez, C., & Galán-Marín, C. (2021). Assessing the impact of courtyards in cooling energy demand in buildings. *Journal of Cleaner Production*, 320(August). <https://doi.org/10.1016/j.jclepro.2021.128742>

- Sendra, J. J., Domínguez-Amarillo, S., Bustamante, P., & León, A. L. (2013). Energy intervention in the residential sector in the south of Spain: Current challenges. *Informes de La Construcción*, 65(532), 457–464. <https://doi.org/10.3989/ic.13.074>
- Seo, D., Huang, Y. J., & Krarti, M. (2010). Impact of typical weather year selection approaches on energy analysis of buildings. *ASHRAE Transactions*, 116 PART 1, 416–427.
- Serrano-Jiménez, A., Lizana, J., Molina-Huelva, M., & Barrios-Padura, Á. (2019). Decision-support method for profitable residential energy retrofitting based on energy-related occupant behaviour. *Journal of Cleaner Production*, 222. <https://doi.org/10.1016/j.jclepro.2019.03.089>
- Shen, P., Braham, W., & Yi, Y. (2019). The feasibility and importance of considering climate change impacts in building retrofit analysis. *Applied Energy*, 233–234(October 2018), 254–270. <https://doi.org/10.1016/j.apenergy.2018.10.041>
- Siu, C. Y., & Liao, Z. (2020). Is building energy simulation based on TMY representative: A comparative simulation study on doe reference buildings in Toronto with typical year and historical year type weather files. *Energy and Buildings*, 211. <https://doi.org/10.1016/j.enbuild.2020.109760>
- Stewart, I. D., & Oke, T. R. (2012). Local climate zones for urban temperature studies. *Bulletin of the American Meteorological Society*, 93(12), 1879–1900. <https://doi.org/10.1175/BAMS-D-11-00019.1>
- Taleghani, M. (2014). *Dwelling on Courtyards. Exploring the energy efficiency and comfort potential of courtyards for dwellings in the Netherlands*. Delft University of Technology.
- Toparlar, Y., Blocken, B., Maiheu, B., & van Heijst, G. J. F. (2018). Impact of urban microclimate on summertime building cooling demand: A parametric analysis for Antwerp, Belgium. *Applied Energy*, 228(June), 852–872. <https://doi.org/10.1016/j.apenergy.2018.06.110>
- TRNSYS 18 Technical Documentation. Volume 9: Tutorials. (n.d.).
- Tsoka, S., Tolika, K., Theodosiou, T., Tsikaloudaki, K., & Bikas, D. (2018). A method to account for the urban microclimate on the creation of ‘typical weather year’ datasets for building energy simulation, using stochastically generated data. *Energy and Buildings*, 165, 270–283. <https://doi.org/10.1016/j.enbuild.2018.01.016>
- United Nations. (2015). *Sustainable Development Goal 13. Take urgent action to combat climate change and its impacts (SDG13)*. <https://sustainabledevelopment.un.org/sdg13>
- Vazquez Otero, J. L. (2016). *Análisis de pérdidas energéticas por infiltración de aire. Apeia*.
- Warren, P. R. (1977). Ventilation through openings on one wall only. *International Conference on Heat and Mass Transfer in Buildings*, 189–209.
- Warren, P. R., & Parkins, L. M. (1985). Single-sided ventilation through open windows. *Conference Proceeding Thermal Performance of the Exterior Envelopes of Buildings*, ASHRAE, 20.
- WMO and WHO. (2015). *Heatwaves and Health: Guidance on Warning-System Development* (G. R. McGregor, P. Bessemoulin, K. Ebi, & B. Menne (Eds.); Issue 1142). WMO and WHO. [http://www.who.int/globalchange/publications/WMO\\_WHO\\_Heat\\_Health\\_Guidance\\_2015.pdf](http://www.who.int/globalchange/publications/WMO_WHO_Heat_Health_Guidance_2015.pdf)

- Xu, L., Wang, J., Xiao, F., El-Badawy, S., & Awed, A. (2021). Potential strategies to mitigate the heat island impacts of highway pavement on megacities with considerations of energy uses. *Applied Energy*, 281(October 2020), 116077. <https://doi.org/10.1016/j.apenergy.2020.116077>
- Yang, X., Peng, L. L. H., Jiang, Z., Chen, Y., Yao, L., He, Y., & Xu, T. (2020). Impact of urban heat island on energy demand in buildings: Local climate zones in Nanjing. *Applied Energy*, 260(30), 114279. <https://doi.org/10.1016/j.apenergy.2019.114279>
- Yenneti, K., Ding, L., Prasad, D., Ulpiani, G., Paolini, R., Haddad, S., & Santamouris, M. (2020). Urban overheating and cooling potential in australia: An evidence-based review. *Climate*, 8(11), 1–22. <https://doi.org/10.3390/cli8110126>
- Zamani, Z., Heidari, S., & Hanachi, P. (2018). Reviewing the thermal and microclimatic function of courtyards. *Renewable and Sustainable Energy Reviews*, 93(April), 580–595. <https://doi.org/10.1016/j.rser.2018.05.055>
- Zhou, X., Carmeliet, J., Sulzer, M., & Derome, D. (2020). Energy-efficient mitigation measures for improving indoor thermal comfort during heat waves. *Applied Energy*, 278, 115620. <https://doi.org/10.1016/j.apenergy.2020.115620>